Scripta Materialia 146 (2018) 154–159

Contents lists available at ScienceDirect

Scripta Materialia

journal homepage: www.elsevier.com/locate/scriptamat

Regular article

Microstructure, phase evolution and interfacial effects in a new $Zn_{0.9}Mg_{0.1}TiO_3$-$ZnNb_2O_6$ ceramic system with greatly induced improvement in microwave dielectric properties

Shenhui Lei [a,*], Huiqing Fan [a,*], Xiaohu Ren [a], Jiawen Fang [b], Longtao Ma [a], Hailin Tian [a]

[a] State Key Laboratory of Solidification Processing, School of Materials Science and Engineering, Northwestern Polytechnical University, Xi'an 710072, China
[b] Center for NanoScience (CeNS), Ludwig-Maximilians-Universität München, 80799 Munich, Germany

ARTICLE INFO

Article history:
Received 6 September 2017
Accepted 10 November 2017
Available online xxxx

Keywords:
$Zn_{0.9}Mg_{0.1}TiO_3$-$ZnNb_2O_6$ ceramics
Microwave dielectric properties
Structural evolution
ZnO inhibitor
Interfacial effect

ABSTRACT

$Zn0._9Mg_{0.1}TiO_3$-$ZnNb_2O_6$ (ZMT-ZN) ceramics was synthesized and characterized successfully for the first time, and phase conversion to secondary phases was largely restrained due to the introduction of ZnO nano inhibitors. Excellent microwave dielectric properties and optimal combination were achieved for the ceramics sintered at 1100 °C, i.e., $\varepsilon_r = 27.5$, $Q \times f = 75{,}000$ GHz, $\tau_f = -3.8$ ppm/°C. Particularly, the comparatively insulated interlayers were considered as the key mechanism to impede transportation or transfer of defects and surface polarization charges. Considering the merits of facile, low cost and simple process, this series of ZMT-ZN ceramics are promising new candidates for ultra-low microwave devices.

Due to the growing commercial and scientific interests, the microwave dielectric ceramic with excellent properties has played important role along with the fast development of wireless and satellite communication over the past few decades. Suitable dielectric permittivity ε_r, high quality factor $Q \times f$ or low dielectric loss tan δ, together with good temperature stability τ_f, become the priorities in the mass production of high-speed digital electronic devices especially in the field of wireless communication, for examples, resonator, filter, duplexer, multiplexer, electro-magnetic interference (EMI) filter, patch antenna, global position system (GPS) antenna active module [1–3]. At the same time, the ultra-low loss or ultra-high quality factors ($Q \times f > 40{,}000$ GHz), good temperature stability with a near-zero temperature coefficient of resonance frequency (TCF), takes the position of the top priority to retain maximum signal intensity as well as frequency resolution and adapting to environmental temperature changes [4]. Usually, the TCF of microwave dielectric materials for high-resolution application is required below ±10 ppm/°C. Thus, $ZnNb_2O_6$ based ceramics (ZN) attract much attention for their extremely high Q value. However, the relatively low dielectric permittivity (around 20) and poor temperature stability ($\tau_f \sim -56$ ppm/°C) hinder their application in large-scale production and the future of miniaturization [5–6]. Meanwhile, $ZnTiO_3$ based ceramics possess relatively high dielectric permittivity that could be ascribed to the large electronic polarizability of Ti ions [7–8]. Especially, $Zn_xMg_{1-x}TiO_3$ (ZMT) ceramic is a strong performer due to the excellent properties [9] ($Q \times f > 60{,}000$ GHz, $0.1 \le x \le 0.4$). As a result, the combination of ZN and ZMT ceramics could achieve a balanced properties for various applications.

However, according to our works and related references, the ZMT ceramic is easy to transform into the second phase $(Zn, Mg)_2TiO_4$ over 950 °C in the conventional sintering process [9–11]. More importantly, the impurity of $ZnTiNb_2O_8$ phase can also be obtained easily as the required densification temperature for ZN ceramic is usually upon 1250 °C. Therefore, the ZMT-ZN ceramics are not able to synthesize in pure phases by using routine approaches, and the secondary phase has turned out to be an inevitable issue for the application. Besides, ZMT ceramics also suffer from the oxygen loss as sintered at high temperature (even as high as 1400 °C for pure $MgTiO_3$ component), which Ti^{4+} might be partially reduced to Ti^{3+} and further increase the dielectric loss.

Moreover, as well known, the structure and composition can effectively modify the properties of materials. And the relationship between structure and microwave dielectric properties needs to be carefully investigated to realize a controllable high performance of the materials. Coincidentally, we successfully achieve pure phase of $Zn_{0.9}Mg_{0.1}TiO_3$ ceramic by innovative introduction of ZnO nano inhibitors which suppress the nucleation and growth of the second phases upon the phase transition temperature. Finally, a series of ZMT-ZN ceramics with excellent properties are prepared, which makes this system promising in the broad application of related electronic devices and components.

* Corresponding authors.
E-mail addresses: leishenhui@163.com (S. Lei), hqfan@nwpu.edu.cn (H. Fan).

https://doi.org/10.1016/j.scriptamat.2017.11.025
1359-6462/

The FE-SEM microstructural photographs (thermal-etched surface) of *x*ZMT-(*1-x*)ZN ceramic specimens sintered at 1100 °C for 3 h are exhibited in Fig. 1 (a–f). Pure ZN ceramic are also sintered at 1100 °C with nano ZnO as a sintering additive, shown in Fig. 1(f). Based on our previous works, pure $ZnTiO_3$ phase could be successfully prepared by an innovative introduction of dispersive nano ZnO inhibitor regions into $ZnTiO_3$ matrix to avoid the formation of nucleation centers of secondary phases as well as to inhibit the migration of phase boundaries [11]. Thus, the phase transition reaction is largely prevented upon the transformation temperature (see the supplemental informations). Here, the pure ZMT phase can also be guaranteed. That is because the $ZnTiO_3$ and $MgTiO_3$ have the same hexagonal perovskite structure in $R\underline{3}$ space group. The results indicate that well-developed microstructures without pores or cracks can be achieved. It reveals that the phase transition happens at $x = 0.3$, from hexagonal to orthorhombic structure, and the two ceramic grains have apparent different morphologies. For $x \le 0.2$, the ZMT is the dominant phase, while ZN phase predominates for $x > 0.7$. And these results are consistent with XRD patterns.

The XRD patterns of *x*ZMT-(*1-x*)ZN ceramics sintered at 1100 °C are shown in Fig. 1(g). It indicates that main phases are columbite $ZnNb_2O_6$ phase and hexagonal $ZnMgTiO_3$ phase according to composition and peak position. There are no peaks indexed to the impurities: ixiolite $ZnTiNb_2O_8$ or inverse spinel type $(Zn, Mg)_2TiO_4$, suggesting that nano ZnO particles successfully prevent the decomposition of $ZnMgTiO_3$ phase in the whole sintering process. In the meantime, based on related references and our experimental data, the $Zn_yMg_{1-y}TiO_3$ ceramics (*y*, 0.1–0.4) could achieve excellent performances, as a quality factor $Q \times f$ over 60,000 GHz. However, they all possess negative TCF parameters ($\tau_f \sim -80$ ppm/°C) except for $y \le 0.1$. The τ_f value could reach $+25 \sim +30$ ppm/°C under different processing conditions, usually due to the lowered distortion and titling of TiO_6 octahedrons. Thus, the only possible way to obtain a near-zero TCF as well as perfect performance is to combine the strengths of $Zn_{0.9}Mg_{0.1}TiO_3$ and $ZnNb_2O_6$ ceramics in the real production.

As aforementioned, the $ZnMgTiO_3$ phase could be thoroughly transformed into $(Zn, Mg)_2TiO_4$ second phase over 945 °C [9,10], resulting in largely reduced *Q* factors. However, in Fig. 1, the pure phase of ZMT ceramics could be indexed with characteristic reflections of (104) and (110) peak at 32° and 35°, respectively. The ZN ceramic also matches well with recorded PDF card (JCPDS #37-1371), and the characteristic peaks (031) and (131) are located at 24° and 30°, respectively. All XRD peaks shift to lower angle with increasing amount of $ZnNb_2O_6$ phase due to the larger size of unit cells for orthorhombic $ZnNb_2O_6$ phase, as well as a larger ionic size of Nb^{5+} to Ti^{4+} ions (0.64 to 0.605 nm) [12–15].

Theoretical density and relative density are calculated from the atomic weight and crystal structure by Eq. (2)–(4) [16],

$$\rho_{theoretic} = \frac{ZA}{V_c N_A} \tag{2}$$

$$\rho_{relative} = \frac{\rho_{real}}{\rho_{theoretic}} \tag{3}$$

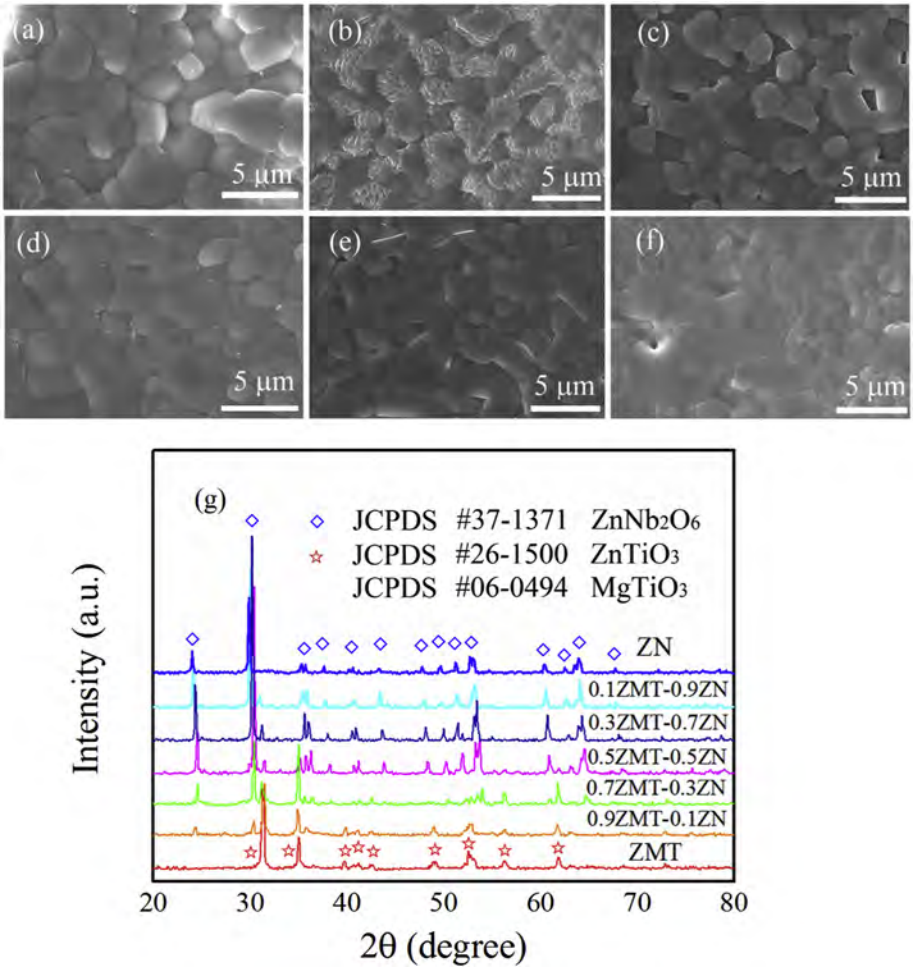

Fig. 1. FE-SEM micrographs of *x*ZMT-(*1-x*)ZN ceramics, thermal-etched surface with different composition (a) $x = 0.9$, (b) $x = 0.7$. (c) $x = 0.5$, (d) $x = 0.3$, (e) $x = 0.1$, (f) $x = 0.9$. (g) XRD patterns of *x*ZMT-(1-*x*)ZN ceramics as a function of *x* (0, 0.1, 0.3, 0.5, 0.7,0.9, 1.0).

$$\rho = \frac{\omega_1 + \omega_2}{\omega_1/\rho_1 + \omega_2/\rho_2} \tag{4}$$

where Z is number of atoms in unit cell, A is atomic weight (g/mol), Vc is volume of unit cell (cm^3), N_A is Avogadro number (mol^{-1}). ω_1 and ω_2 are the weight fraction of ZMT and ZN ceramics, respectively.

The corresponding theoretical density and relative density are demonstrated in Fig. 2(c). Densification of ceramics is the critical extrinsic factor determine dielectric performance of microwave dielectric materials. There are no significant changes observed in dielectric properties among different composition (as their relative densities can all achieve 97%–98%), though a reduction of relative density happens at $x = 0.3$ that is due to the growing interfaces and grain boundaries related with the transition process from hexagonal to orthorhombic structure. Thus, the stable and reliable dielectric properties can be closely associated with intrinsic factors, microstructures. From Fig. 2(d–f), it's clearly observed that the significant differences between the TEM images with or without ZnO nano inhibitors regions. The nano ZnO inhibitors can enforce the elimination of the nucleation centers and suppress the mass transfer to the secondary phases, i.e., $(Zn, Mg)_2TiO_4$ and $ZnTiNb_2O_8$ (normally this process is governed by the migration of Ti ions). Therefore, the pure ZMT phase and ZN phase can be achieved above the phase transition temperature, and these results can also be proved by the energy dispersive spectroscopy (EDS) image and selected area electron diffraction (SAED) patterns in Fig. 2.

To study the conductivity mechanisms of ZMT-ZN ceramics and reveal the deep reasons of highly improved dielectric properties, variable frequency impedance analysis were carried out in air at 300 °C, exhibited in Fig. 3(a,b). For the ceramics, impedance data shows the two arcs are associated with two different main resistances R_g and R_{gb}, which stands for ceramic grains and grain boundaries, respectively. Replotting

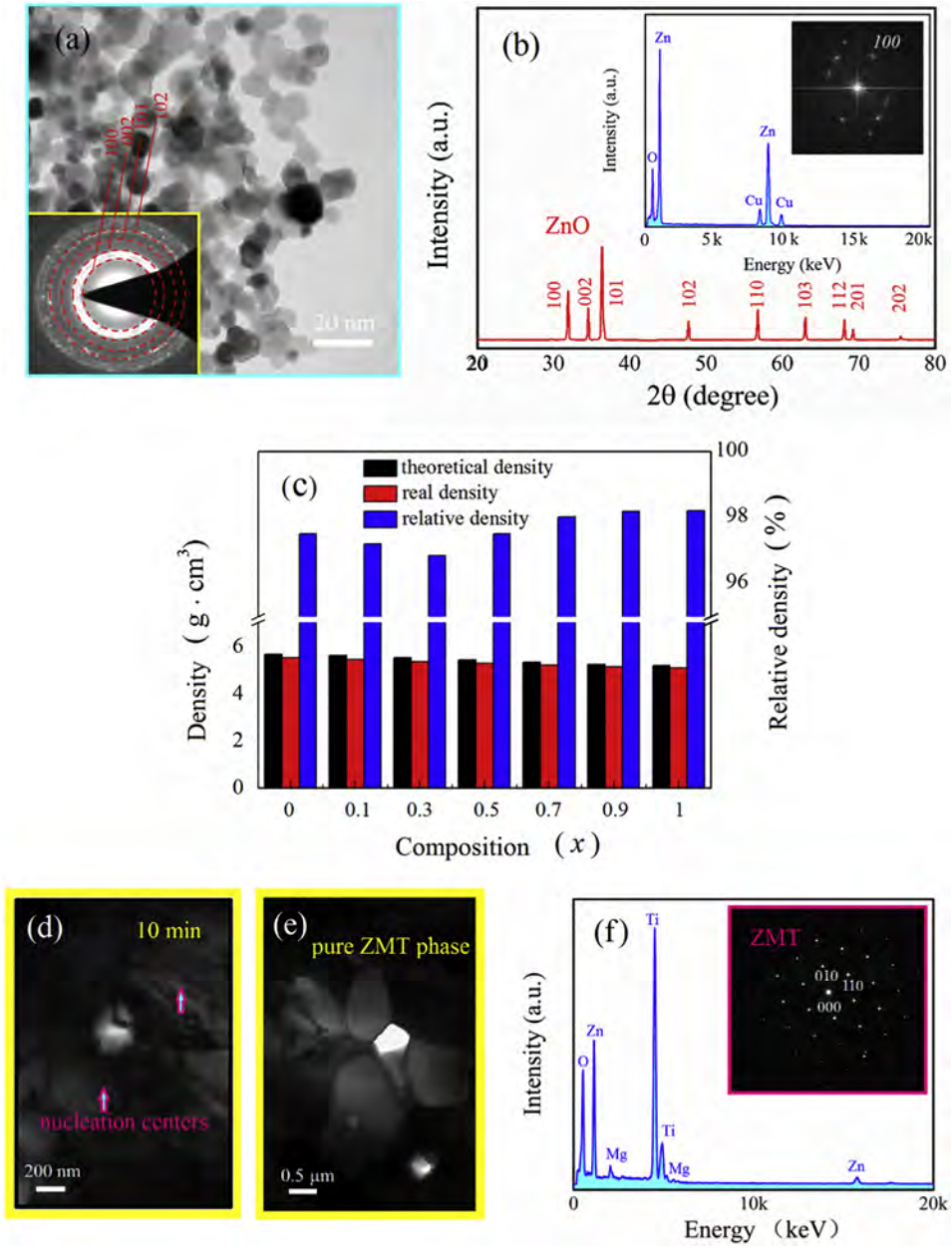

Fig. 2. (a) Transmission electron microscopic micrographs of nano ZnO particles, (b) XRD pattern and EDS graph of ZnO particles, inset is the FFT image of a ZnO particle, (c) theoretical and relative density of the *x*ZMT-(*1-x*)ZN ceramics to different composition listed in the color bars. (d) The TEM image for the ZMT ceramic without nano ZnO inhibitor, and the nucleation centers for the second phase are clearly observed in 10 min sintered samples, (e) the TEM images for pure ZMT phase with ZnO nano inhibitors sintered for 3 h, (f) EDS graph of ZMT phase, inset is the SAED patterns for pure ZMT phase in hexagonal structure by (001) zone axis.

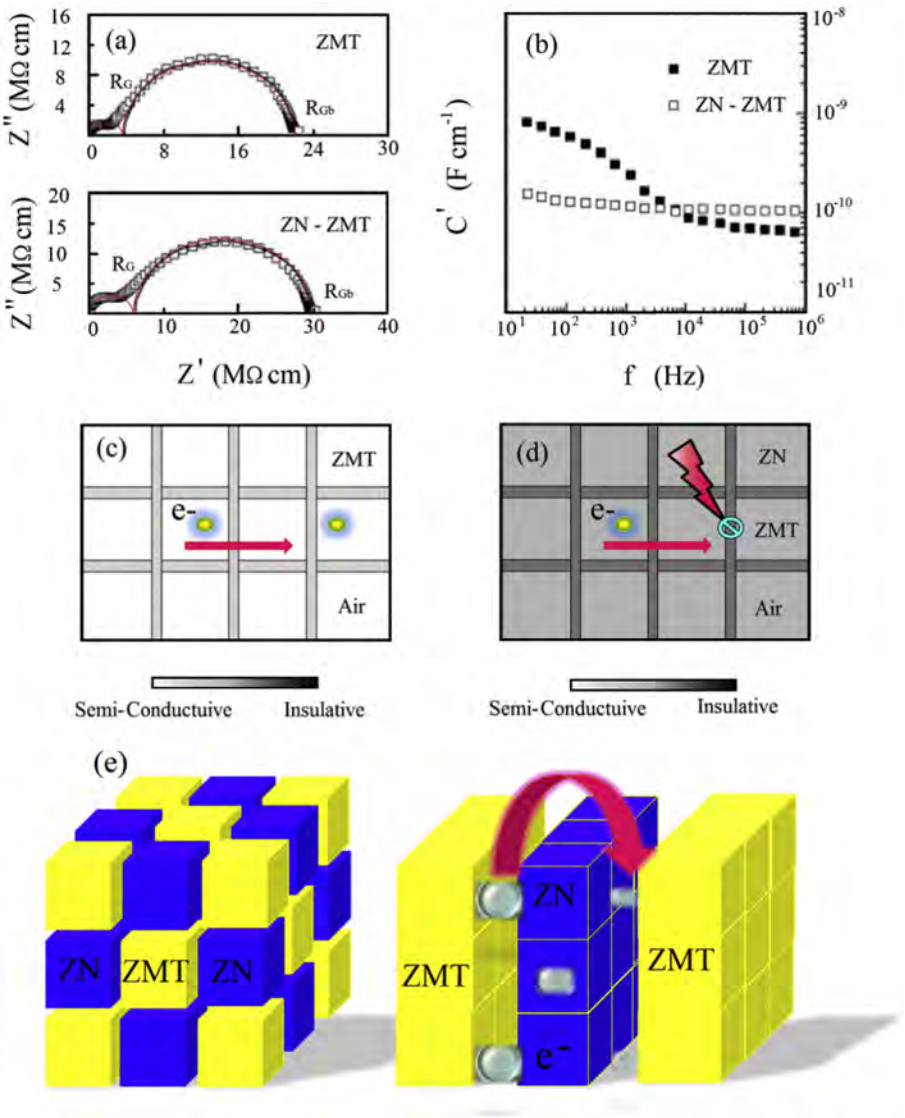

Fig. 3. (a) Impendence complex plane plots and (b) C' spectroscopic plot for ZMT-ZN ceramics, (c) and (d) schematic electrical microscopes image of relatively insulative interfaces in ZMT-ZN based ceramics in air, (e) schematic image of inhibited electron hopping in ZMT-ZN based ceramics.

the spectroscopic data of capacitance C' against the frequency, inclined capacitance curve become more gentle downslope. It is attributed to the contribution of the inner interfaces or phase boundaries by introducing in more insulative $ZnNb_2O_6$ phase. Fig. 3(c) suggests the existence of different mechanism of conductivity for electrons or holes in the ceramics. The creation of oxygen vacancy is believed to be associated with the oxygen loss in the high temperature sintering process, depicted in the Formula (5) and (6). The electrons can be created both through the oxygen loss reaction or the reduction of Ti^{4+} to Ti^{3+} as expressed as follows [17]:

$$O_o^x \leftrightarrow V_o^{\cdot\cdot} + 2e' + \frac{1}{2}O_2 \tag{5}$$

$$2Ti_{Ti}^x + O_o^x \leftrightarrow 2Ti_{Ti}' + V_o^{\cdot\cdot} + \frac{1}{2}O_2 \tag{6}$$

$$Ti_{Ti}^x + e' \leftrightarrow Ti_{Ti}' \tag{7}$$

The defect carriers and polarized dipoles usually induce the polarization relaxation and increase the dielectric loss (mostly the conductive loss and dielectric relaxation loss). The main defects are commonly electrons and oxygen vacancies at room temperature. As the introduction of factitious interfaces, electron hopping (between Ti^{4+} and Ti^{3+}) and electric transfer are largely suppressed (see Fig. 3). Thus, the frozen defects, elimination of precipitation and diffusion of secondary phases result in the much improved $Q \times f$ values. This contribution can also compensate the theoretical weaken properties caused by density reduction. It's worth mentioning that, the ZMT-ZN ceramic with $x = 0.9$ has a comparable quality factor $Q \times f$ to those ZN-dominant ceramics, validating the foregoing analysis.

As depicted in Fig. 4, nano ZnO particles serve as different roles in ZMT-ZN ceramics facilitating the much improved properties in this system. For ZMT component ($Zn_{0.9}Mg_{0.1}TiO_3$ phase with hexagonal symmetry) [18,19], the ZMT-ZN ceramics are prone easily to form the secondary phases $(Zn, Mg)_2TiO_4$ and $ZnTiNb_2O_8$ over 950 °C [20,21], which results in grievous performance deterioration. However, in this work, the ZMT phase can be stabilized by nano ZnO inhibitors due to the removal of nucleation centers of secondary phases and resistance of mass transfer. During the whole sintering process the dynamic pure phase can be guaranteed by nano ZnO buffer regions even upon the phase transition temperature (at 1100 °C), shown in Fig. 4(a). On the other hands, the ZN ceramic also gets higher densification by nano ZnO as a sintering aids at 1100 °C (the normal sintering temperature

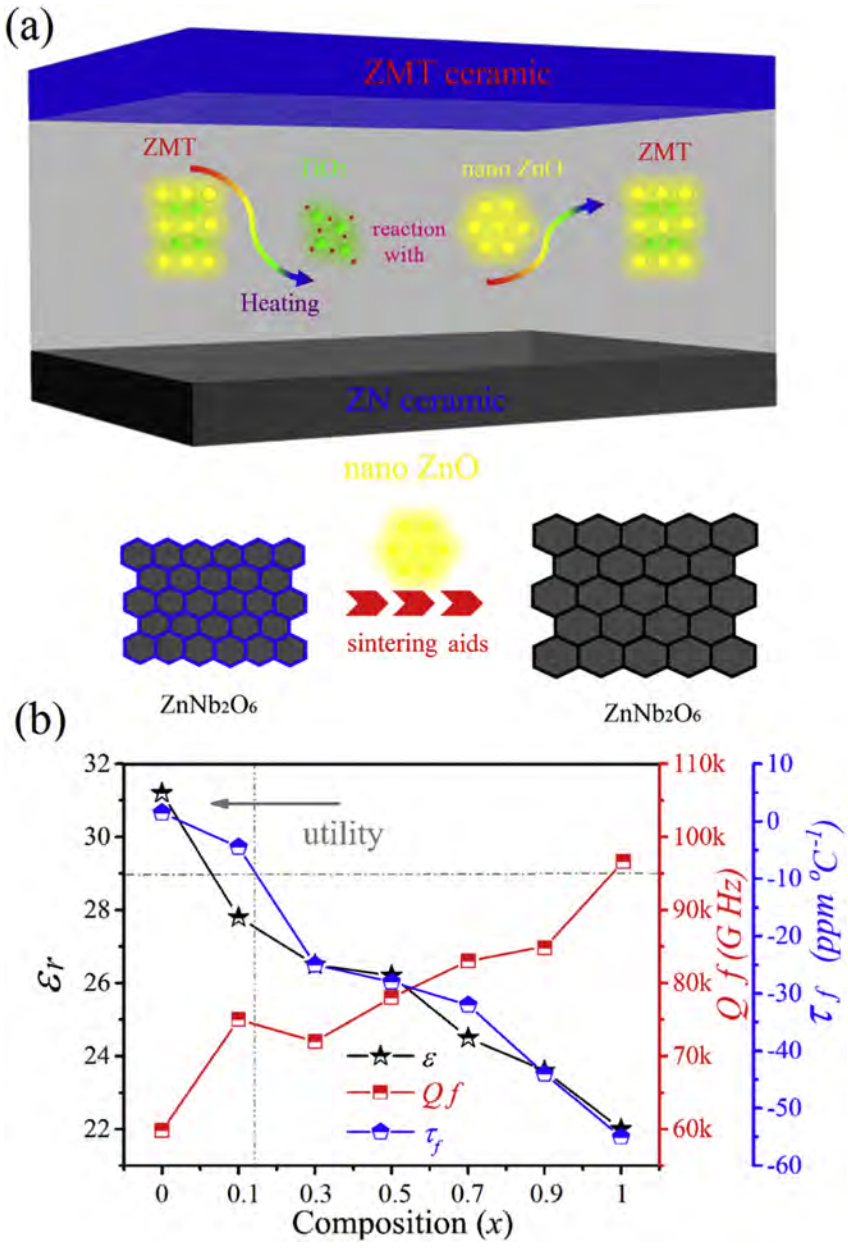

Fig. 4. (a) Schema of mechanisms related with ZMT and ZN ceramic accompanied by nano ZnO precursor, respectively. (b) Microwave dielectric properties of ZMT-ZN based ceramics with different composition *x*. The dielectric permittivity ε, quality factor $Q f$ (GHz) and temperature coefficient τ_f (ppm/°C) are depicted with different symbols.

of ZN ceramics is over 1250 °C). The lower sintering temperature will bring in less defects such as oxygen vacancies. Thus, pure phase and homogenous microstructure of high quality are believed as fundamental causes of the obtained excellent microwave dielectric properties in ZMT-ZN ceramics. The corresponding microwave dielectric properties of ZMT-ZN ceramics are listed in Table. 1. This new ZMT-ZN ceramics

Table. 1
Performance of $ZnTiO_3$, $MgTiO_3$ based materials using different preparation methods.

Methods	Composition	Impurities	ε_r	$Q \times f$ (GHz)	τ_f (ppm/°C)	reference
Sol-gel	$ZnTiO_3$	Zn_2TiO_4	19	35,000	−55	[18]
Hydrothermal	$ZnTiO_3$	Zn_2TiO_4	25	–	18	[19]
Solution	$ZnTiO_3$	Zn_2TiO_4	26	32,000	−90	[20]
Solid state	$Zn(Mg)TiO_3$	$(Zn,Mg)_2TiO_4$	25	40,000	0	[17]
Solid state	$ZnTiO_3$	Zn_2TiO_4	23	25,000	15	[16]
Solid state	$MgTiO_3$	No	16.55	139,350	−49	[21]
Solid state	$ZnTiO_3$	No	31.2	59,800	1.5	[11]
Solid state	$ZnNb_2O_6$	No	25	87,300	−56	[22]
Solid state	ZMT-ZN	$(Zn,Mg)_2TiO_4$ + $ZnTiNb_2O_8$	25–26	14,000–25,000	−80	[23]
Solid state	ZMT-ZN	No	27.5	75,000	−3.8	This work

achieve both excellent integrated properties as well as low sintering temperature in the ZnO-TiO_2, MgO-TiO_2, ZnO-MgO-TiO_2 and ZnO_2-Nb_2O_5 material systems, showing a potential application of these materials as broad microwave circuit components in related fields.

In summary, $x Zn_{0.9}Mg_{0.1}TiO_3$ ~ $1\text{-}x ZnNb_2O_6$ (ZMT-ZN) ceramics in pure phases are successfully synthesized by simple solid state method for the first time. XRD and SEM results reveal the dense microstructure of high quality without impurities upon the phase transition temperature. This system presents adjustable dielectric permittivity as well as outstanding temperature stability in wide compositional region and can be easily fabricated. Excellent microwave dielectric properties (especially ultra-high $Q \times f$ value and near zero temperature coefficient of resonance frequency) are realized in the present ceramics with $\varepsilon_r =$ 27.5, $Q \times f =$ 75,000 GHz, $\tau_f = -3.8$ ppm/°C, which are outstanding among the $ZnTiO_3$, $MgTiO_3$ and $ZnMgTiO_3$ systems, and almost compete with $Ba(Mg_{1/3}Ta_{2/3})O_3$ ceramic at a much lower temperature (1000–1100 °C). During the whole sintering process the dynamic pure phase can be guaranteed by nano ZnO inhibitor even upon the phase transition temperature. As the introduction of factitious insulative interfaces, electron hopping (between Ti^{4+} and Ti^{3+}) and carrier conduction are largely suppressed. Thus the pure phase and homogenous microstructure in high quality are believed as deep reasons for the excellent microwave dielectric properties of ZMT-ZN ceramics. Given its easy fabrication, high efficiency, low-cost and environmental friendliness, the ZMT-ZN ceramics have great potential for exploitation in ultra-low loss microwave components and devices.

Acknowledgement

This work was supported by the National Natural Science Foundation (51672220), the 111 Program (B08040) of MOE, the National Defense Science Foundation (32102060303), the Xi'an Science and Technology Foundation (CXY1706-5, 2017086CGRC049-XBGY005), the Shaanxi Provincial Science Foundation (2017KW-018), and the NPU Gaofeng Project (17GH020824) of China.

Appendix A. Supplementary data

Supplementary data to this article can be found online at https://doi.org/10.1016/j.scriptamat.2017.11.025.

References

[1] J. Guo, H.Z. Huo, A.L. Baker, M.T. Lanagan, E.R. Kupp, et al., Angew. Chem. Int. Ed. 55 (2016) 1–6.
[2] Y.H. Jung, J. Lee, Y. Qiu, N. Cho, S.J. Cho, H. Zhang, Adv. Funct. Mater. 26 (2016) 4635–4642.
[3] J. Dhanya, A.V. Basiluddeen, R. Ratheesh, Scr. Mater. 132 (2017) 1–4.
[4] S.H. Lei, H.Q. Fan, W.N. Chen, Z.Y. Liu, M. Li, J. Am. Ceram. Soc. 100 (2017) 235–246.
[5] H. Li, Q. Li, J. Zhang, S. Huang, Y. Yu, J. Zheng, J. Eur. Ceram. Soc. 36 (2016) 2513–2518.
[6] B. Qu, H. Du, Z. Yang, Q. Liu, J. Am. Ceram. Soc. 100 (2017) 1517–1526.
[7] C.F. Tseng, J. Eur. Ceram. Soc. 34 (2014) 3641–3648.
[8] M.A. Khan, T.P. Comyn, A.J. Bell, Appl. Phys. Lett. 91 (2007), 032901.
[9] H. Kim, S. Nahm, J. Byun, J. Am. Ceram. Soc. 82 (1999) 3476–3480.
[10] A. Chaouchi, S. Marinel, M. Aliouat, S. Astorg, J. Eur. Ceram. Soc. 27 (2007) 2561–2566.
[11] S.H. Lei, H.Q. Fan, X.H. Ren, J.W. Fang, L.T. Ma, Z.Y. Liu, J. Mater. Chem. C 5 (2017) 4040–4047.
[12] W.D. Kingery, H.K. Bowen, D.R. Uhlmann, Introduction to Ceramics, 2nd ed. Wiley, New York, 1976.
[13] K. Xu, J. Li, J.G. Wu, X.X. Zhang, D.Q. Xiao, et al., Adv. Mater. 28 (2016) 8519–8523.
[14] B.W. Hakki, P.D. Coleman, IEEE Trans. Microw. Theory Tech. 8 (1960) 402–410.
[15] R.D. Shannon, Acta Cryst. A 32 (1976) 751–767.
[16] A. Chaouchi, S. Marinel, M. Aliouat, S. d'Astrog, J. Eur. Ceram. Soc. 27 (2007) 2561–2566.
[17] Y.H. Yu, M. Xia, Mater. Lett. 77 (2012) 10–12.
[18] X.C. Liu, Mater. Lett. 80 (2012) 69–71.
[19] C.F. Shih, W.M. Li, M.M. Lin, K.T. Hung, J. Electrochem. Soc. 156 (2009) E13–E17.
[20] L. Bobowaka, A. Opasinska, A. Wypych, P. Wokcienchowski, Mater. Chem. Phys. 134 (2012) 87–92.
[21] S.K. Thatikonda, D. Goswami, P. Dobbidi. Ceram. Int. 40 (2014) 1125–1131.
[22] J. Wang, Z. Yue, Z. Gui, L. Li, J. Mater. Sci. 40 (2005) 6581–6583.
[23] X.C. Liu, J.P. Deng, J. Mater. Sci. Mater. Electron. 33 (2012) 506–510.